Final Report

Detecting gravitational wave transients from unmodeled sources

Enia Xhakaj,[1]
Mentors: Jonah Kanner,[2] and Alan Weinstein[2]
[1)] *Lafayette College, Easton, PA*
[2)] *California Institute of Technology, Pasadena, CA*

(Dated: 26 September 2015)

With the recent installation of the Advanced LIGO detectors in Hanford and Livingston, the sensitivity of detecting gravitational waves (GWs) has improved significantly. However, especially for unmodeled sources, it is still difficult to distinguish signals from instrumental noise with high confidence. The recent science and engineering runs suggest that apart from stationary Gaussian noise there are other instrumental artifacts, called "glitches" that impose a challenge in recovering signals. The BayesWave Pipeline presents a novel way to approach this problem. BayesWave uses modern statistical methods to model the data as containing signals or glitches and attempts to calculate the evidence for each of the two competing models. In this project, we test the pipeline's performance in recovering injected signals added to initial LIGO data. We run BayesWave as a follow-up to coherent WaveBurst (cWB), which is the primary analysis pipeline for identifying burst signals in noisy data from the LIGO detectors, and we compare the efficiency for confident burst detection of cWB alone with that of the combined pipeline.

I. INTRODUCTION

Recently the Advanced LIGO interferometers in Hanford and Livingston had their fist engineering runs while their first observations are scheduled to begin in mid-September 2015. Advanced LIGO will approach the designed sensitivity over the next few years, and will likely observe GWs by 2020. In addition to detector upgrades, improvements to data analysis algorithms are also ongoing. For example, identifying unmodeled transient sources (Bursts) at high statistical confidence remains challenging. This is due to instrumental components that introduce noise into the data. Apart from stationary Gaussian noise, the latest engineering runs have shown that there are also instrumental noise transients, called "glitches". These tend to be loud and difficult to separate from astrophysical signals, especially in Burst searches.

The BayesWave pipeline was developed by Cornish and Littenberg[1], targeting the detection of core collapse supernovae, intermediate-mass black hole mergers, and unexpected short duration signals. The name BayesWave comes from *Bayesian* and *Wavelets*, suggesting that this algorithm uses Bayesian Statistics to distinguish between signals and glitches. BayesWave fits the data with three competing models: the data are consistent with Gaussian noise, the data contain a glitch, or the data contain an astrophysical signal. Both the glitch and signal models are represented by sums of Morlet-Gabor Wavelets[2] which not only provide a compact way of representing the models, but also make the analysis easier by allowing to work in the Fourier domain. The stationary Gaussian Noise is modeled by adopting the *BayesLine* spectral whitening algorithm which fits the data as a combination of a smooth noise curve and a collection of Lorentzians[3].

The model selection and waveform reconstruction is done by implementing a trans-dimensional Reversible Jump Markov Chain Monte Carlo algorithm[4], which varies both the number of parameters needed to build the models and their values. This allows BayesWave to find a balance between model complexity and the precision of waveform estimation.

II. MOTIVATION

Previous burst searches have shown a "tail" of glitches in the coincident event background (modeled using time-slides)[5], making it difficult to find any signals with high confidence (false positive rate less than 1 in 100 years). Based on previous analysis, we believe that BayesWave can succeed in extracting astrophysical signals from glitches and other instrument noise with a higher confidence. In this project, we are using various analytic tools to test the BayesWave pipeline on the data from the last science run of initial LIGO (S6). The results of this study will inform analysis plans for Advanced LIGO.

III. METHODS

A. The Hierarchical Pipeline

In order to test the performance of BayesWave, we introduced a hierarchical pipeline that runs cWB as the first stage of the analysis and BayesWave as a follow-up. cWB is a pipeline used in previous analysis that addresses short duration, low-frequency burst searches, with a bandwidth ranging from 32Hz to 2048 Hz. The detection statistic of cWB is ρ, which is scales proportionally with the Signal to Noise Ratio (SNR). One of the most important characteristics of this pipeline is that it can process the data using low computational power by applying Data Quality cuts[6] to look for glitches. The process of using the hierarchical pipeline speeded up the analysis as well as maintained the main features of

BayesWave that we aimed to test.

B. Background and Injections

In this study, we used 50 days worth of LIGO S6 data collected by the Hanford and Livingston interferometers. Ad Hoc signals, including Sine Gaussians, Gaussians, and White Noise Bursts (see Figure 1) with different parameters were injected to this data set. In order to measure the probability of falsely considering a glitch as a signal, the background data set was created. This data set consisted of 70.1 years worth of data, that were provided by time-shifting the interferometer data by 500 lags to minimize the chance of having any astrophysical signal in the background. As a result, the new data consisted solely of glitches and gaussian noise.

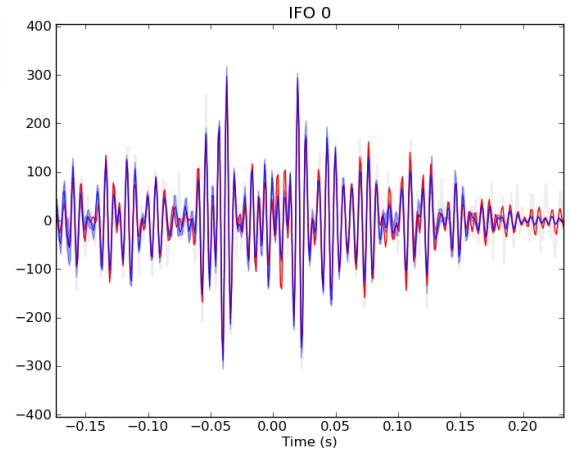

FIG. 1. Example of a White Noise Burst injection represented in the time domain. White Noise Bursts are random waveforms with fixed duration and bandwidth.

C. Running BayesWave and Data Analysis

We used the background triggers produced by running cWB to estimate the degree of confidence with which the combined pipeline can differentiate between a signal and a glitch. Once these triggers ran through BayesWave, we measured the False Alarm Rate (FAR) as a function of the detection statistic, which is the Signal-to-Glitch Bayes Factor. In addition, we studied how well the combined pipeline could recover the injected signals by processing different sets of cWB triggers with BayesWave. These sets of triggers included 1300 Sine Gaussian injections, with quality factors from Q = 3 to Q = 100, and central frequencies from 70 Hz to 253Hz, as well as 770 white noise bursts injections with central frequency ranging from 250Hz to 1000Hz, and bandwidth of 100Hz and 1000Hz. We compared the performance of the combined pipeline with that of cWB alone by analyzing the processed results with different tools like efficiency and Receiver Operating Characteristic (ROC) curves, scatter plots, etc. In addition, we also studied how precisely BayesWave could reconstruct the parameters of the injected signals.

IV. PROGRESS

A. Parameter Recovery

We ran BayesWave through 255 Sine Gaussian simulated signals with a central frequency of 153 Hz and a quality factor of 8.9. Once these injections were processed we tested how well BayesWave estimated the recovered signal parameters, including here central time, central frequency, bandwidth, and duration.

We plotted histograms of the recovered parameters for one of the detectors (left panel of Figure 2). The values on the x-axis are calculated in the following way:

$$x = \frac{p_{mode} - p_{injected}}{\sigma_{90\%}}$$

where p_{mode} is the modal value of the parameters recovered, $p_{injected}$ is the value of the parameter in the simulated signal and $\sigma_{90\%}$ is an estimate of the 90% confidence interval of the recovered parameters. Ideally, if BayesWave had correctly recovered the signal the histograms would be peaked at 0, and 90% of the recovered parameters would be positioned between -1 and 1. Based on our calculations, BayesWave succeeded in recovering a range of 80% to 95% of the injected parameters.

In addition, we ran 200 injections of White Noise Bursts with Central Frequency = 100Hz, Bandwidth = 100Hz and followed the same analysis as above. The right panel of figure 2 shows an example of the histograms for the distribution of the recovered parameters. Unlike the histograms for the parameter recovery of the Sine Gaussian injections, the White Noise Burst histograms are sharply peaked at 0 and do not show a normal Gaussian distribution. Moreover, they have a lower recovery range, that varies from 70% to 85 %. We repeated the same study with other types of Sine Gaussian and White Noise Burst injections and concluded that there was not an obvious pattern that could predict the distribution of the recovered parameters regardless of the waveform. To explore this even more, we analyzed our data using Probability-Probability (PP) plots. The PP plots describe the fraction of the simulated signals whose injected parameter falls into a given confidence interval as a function of the interval itself. Figure 3 shows P-P plots for the Sine Gaussian injections with Central Frequency of 153 Hz and Q = 8.9 (blue) and White Noise Burst injections of Central Frequency = 100 Hz and Bandwidth = 100 Hz (green). Ideally, this would show a curve with

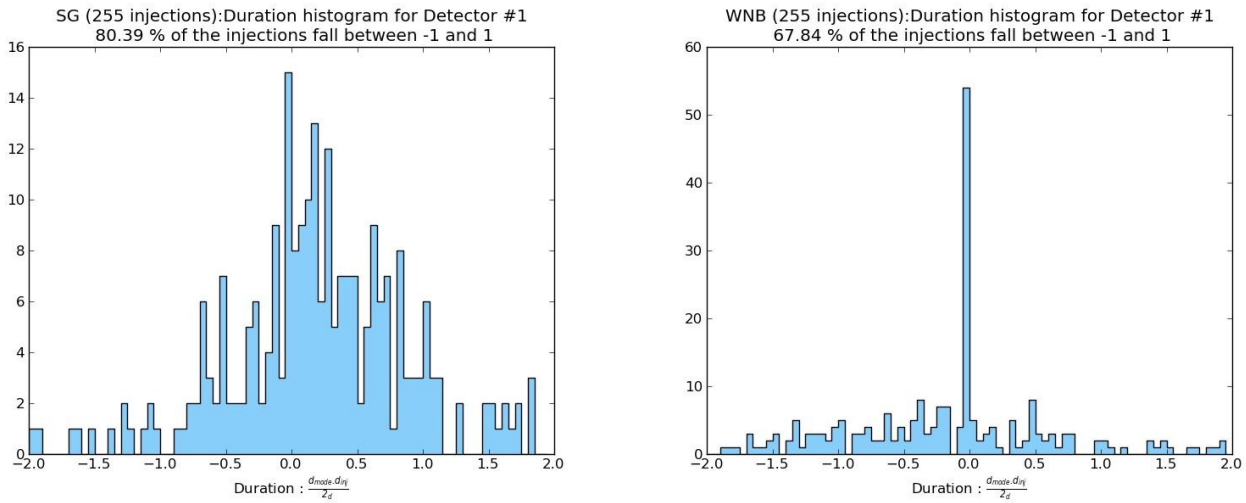

FIG. 2. Example of histograms showing how well BayesWave can recover the parameters of simulated signals of Sine Gaussian (left) and White Noise Bursts (right). Both of the plots show the distribution of one (Duration) of the four different parameters. For the Sine Gaussian waveforms, the distribution of the recovered parameters has a normal Gaussian shape, while, for the White Noise Bursts, this distribution is sharply peaked at 0.

a slope of 1 that passes through the origin. However, our PP plots had a "U-shaped curvature" that is more evident for the duration of the white noise bursts. Notice that for a U-shaped curve the slope increases as we go to higher confidence intervals, which means that the parameter recovery distribution is skewed to the right. As such BayesWave is recovering more injections at the higher confidence intervals. Another way to interpret this is that the posteriors that BayesWave is building are too "thin" in that they slightly include the injected value. These results also agree with the histograms that we introduced before for the white noise burst injections (right panel of figure 2). Since the posteriors are too thin they can either estimate the injected value precisely or miss it completely; this made the histograms for white noise bursts be sharply peaked at 0 and at the same time have a low recovery range. As a result of this study, there must be an issue with the way that BayesWave is estimating the parameters for complex injections like white noise bursts. This might be because of the use of an insufficient number of wavelets to fit the data, an inaccurate prior etc. However, this remains an open question.

B. Overlap

In a range from 0 to 1, the *overlap* shows how well BayesWave is able to recover the waveform of an injection and is calculated by using the following formula:

$$\langle a|b\rangle = \int a(f)b^*(f)df$$

where a is the recovered waveform, b is the injected waveform, f is the frequency, and a, b are both normalized. In figure 4, we plotted the network overlap as a function of the network SNR, for Sine Gaussian and White Noise Burst injections with Network SNR lower than 80. For both the Sine Gaussians and the White Noise Bursts, the overlap improves with the increase of SNR. BayesWave recovers Sine Gaussians more precisely due to the fact that Sine Gaussians have the same waveform as Morlet-Gabor wavelets, which BayesWave adopts to fit the data. White Noise Bursts, on the other hand, are more complex, and thus impose a greater challenge for BayesWave in modeling the waveform.

C. Study of the Background

We ran all cWB triggers with $\rho > 8$ from 70.1 years of time-slide data through BayesWave. We replicated the plots of False Alarm Rate (FAR) as a function of threshold statistic for cWB alone (ρ) and the combined pipeline (the Signal-to-Glitch Bayes Factor)[5]. Figure 6 shows the False Alarm curve for cWB. Going to lower FAR values, ρ increases rapidly. We know that ρ is proportional to the SNR and can be calculated by:

$$\rho = \frac{\mathrm{SNR}}{\sqrt{2}}$$

Therefore, the background event that has the lowest FAR ($\mathrm{FAR} = 4 \cdot 10^{-10}\mathrm{Hz}$) will have $\rho = 45$, which corresponds to $\mathrm{SNR} = 64$. This means that cWB would not only reject as a glitch any astrophysical signal that has an SNR lower than 64, but also automatically consider a signal any trigger with an SNR higher than 64. However, these

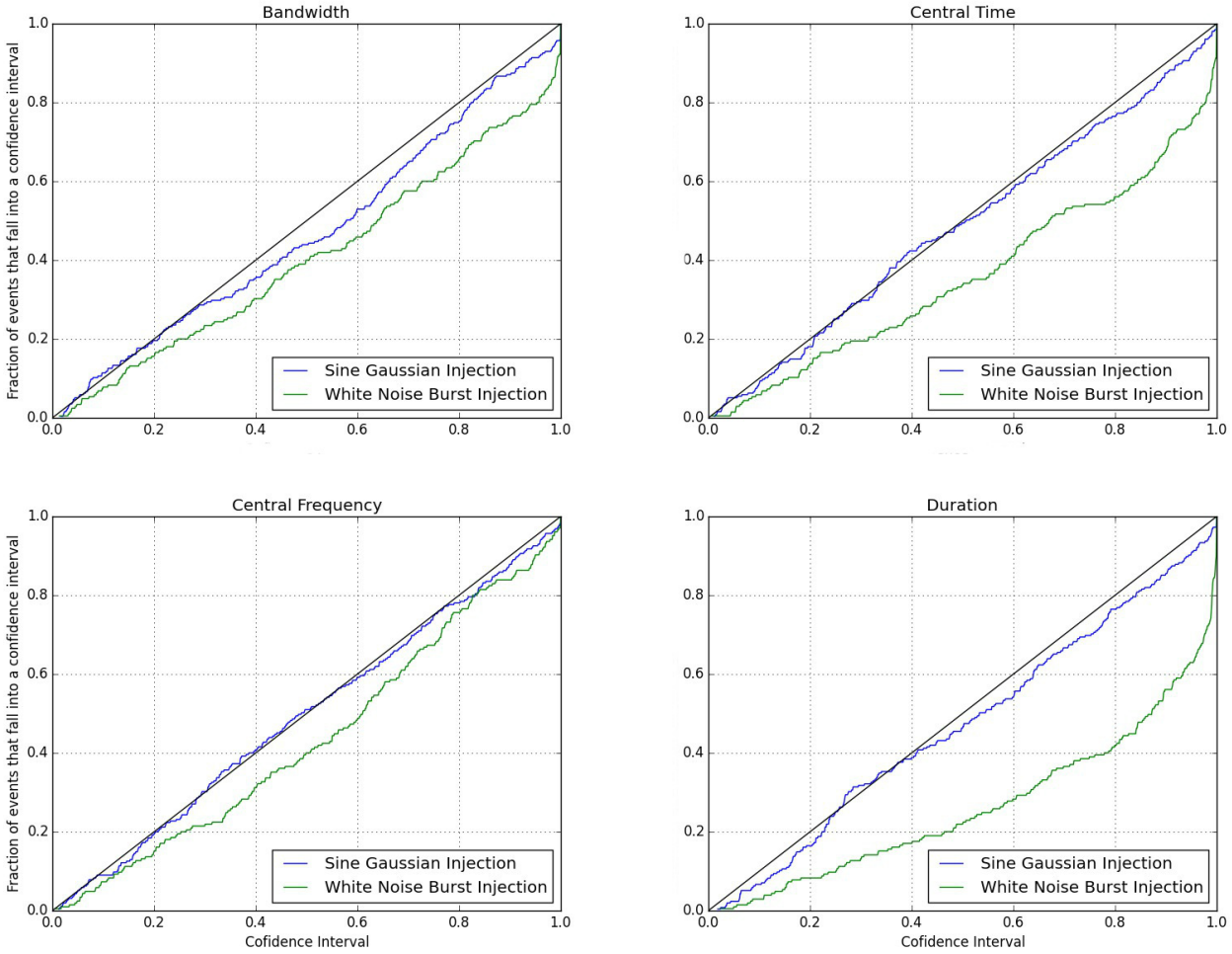

FIG. 3. P-P plots that show how well BayesWave can recover the parameters of the simulated signals. Ideally, the PP curves should be following the black straight line that goes through the origin and has a slope of 1. However, they show a "U-Shaped" curvature.

high SNR triggers are frequently observed as instrumental artifacts in the LIGO detectors and this impedes cWB to claim a high confidence detection. On the other hand, figure 6 shows the same analysis on the background as processed by the combined pipeline. The detection statistic of the combined pipeline is the Bayes Factor, which is scaled as:

$$ln(B_{SG}) \propto N\ln(\mathrm{SNR})$$

where N is the number of wavelets used to reconstruct the model that fits the data, which also represents the model complexity. The fact that $ln(B_{SG})$ scales with N and ln(SNR), instead of SNR alone as in the case of cWB, infers that the combined pipeline stresses more the importance of waveform complexity rather than the trigger's SNR. Following this approach, the combined pipeline can easily recover low SNR GW signals, which were not possible to detect in the case of cWB alone.

D. Detection Efficiency

Once we analyzed the background as processed by each of the pipelines, we studied their ability to recover injected signals by measuring their detection efficiencies. The detection efficiency can be calculated as the ratio of the number of the recovered signals over the total number of injections we run through a given pipeline. We determine the number of recovered signals as the number of triggers that have a detection statistic greater than the threshold we set on the data. In our study, the thresholds for the detection statistics correspond to the FAR of the loudest background event. From the data used to plot figure 5 and 6, the loudest event has a FAR = $4 \cdot 10^{-10}$Hz or once in 70 years. The thresholds for the loudest background event are $\rho = 45$ and Bayes Factor = 16, for cWB and the combined pipeline respectively.

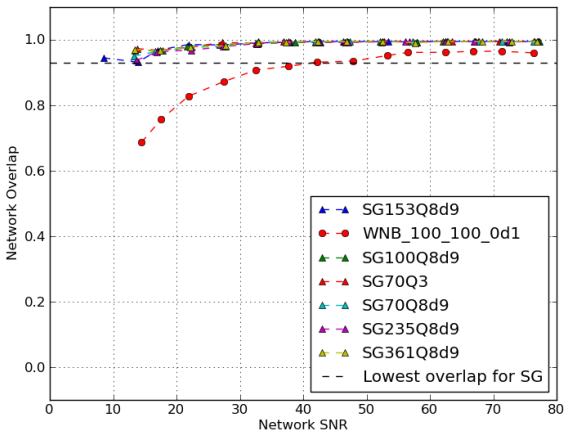

FIG. 4. Network Overlap as a function of Network SNR, for Sine Gaussian and White Noise Burst Injections. In both of the waveforms, the overlap flattens as SNR is increased. The overlap curve for the Sine Gaussians is closer to 1 than that of the white noise bursts. This is because Sine Gaussians have a less complex waveform.

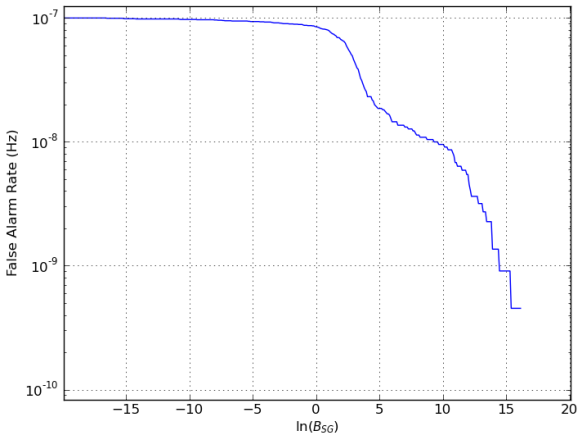

FIG. 6. The False Alarm Rate vs the Signal-to-Glitch Bayes Factor for the background as processed by the combined pipeline. The loudest background event has a $\ln(B_{SG}) = 16$.

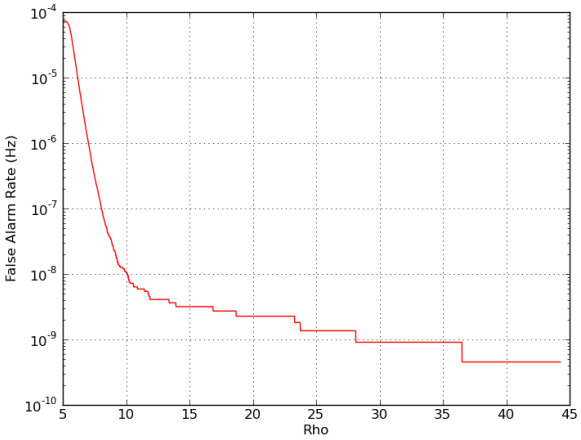

FIG. 5. The False Alarm Rate vs ρ for the background as processed by cWB. The loudest background event has a $\rho = 45$.

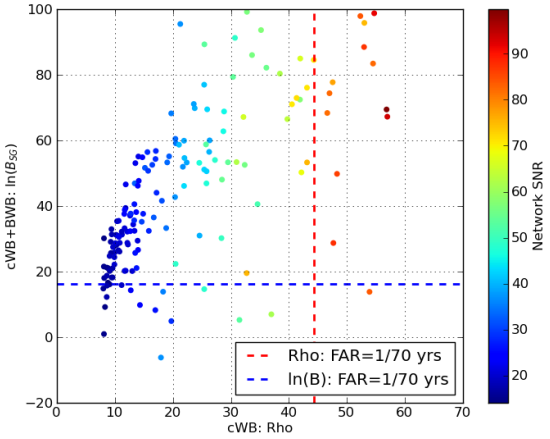

FIG. 7. Scatter plots of ρ dependent on the Signal to Glitch Bayes Factor for White Noise Bursts. The blue and the red dashed lines represent thresholds on the Bayes Factor and ρ respectively corresponding to the loudest background event. Injections positioned in the upper left quadrant were promoted by BayesWave.

1. White Noise Bursts

We ran a total of 770 injections of white noise bursts with different parameters. Figure 7 gives a visual representation of the recovered signals for both cWB and the combined pipeline. In the figure, we plot the Bayes Factor versus ρ, for the injections, color-coded based on their Network SNR. The dashed blue and red lines show the thresholds for ρ and the Bayes Factor respectively, corresponding to the loudest background event, with a FAR of 1 in 70 years. These dashed lines divide the plot into 4 quadrants: The upper-right quadrant includes injections that are recovered from both the pipelines, the upper-left quadrant includes all the injections that are recovered from the combined pipeline but missed from cWB alone. The bottom-left quadrant has all the injections that are missed from both the pipelines, and the bottom-right quadrant shows all the injections that are recovered from cWB but missed from the combined pipeline. For the white noise bursts cWB can recover only high SNR injections. On the other hand, cWB misses all the injections that are in the upper left quadrant, that in-

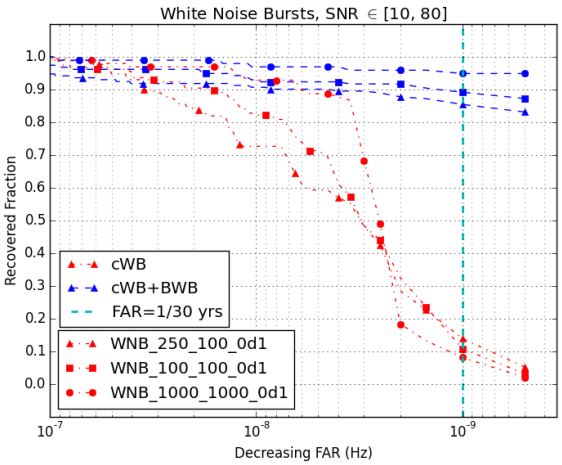

FIG. 8. ROC plots for 3 different sets of White Noise Bursts injections with SNR ranging from 10 to 80. At high confidence regions (on the right of the cyan dashed line), the combined pipeline can recover almost 80% to 90% of the injections.

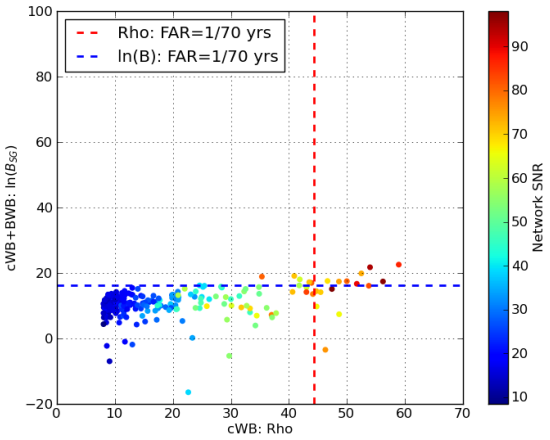

FIG. 9. Scatter plots of ρ dependent on the Signal to Glitch Bayes Factor for Sine Gaussian Injections. In the case of Sine Gaussians both the pipelines perform similarly in the high confidence region.

stead are recovered by the combined pipeline. Therefore, the BayesWave follow-up helps in promoting the injected white noise bursts that, in our plot, are positioned in the upper-left quadrant. This result can be studied more quantitatively showing the ROC plots in Figure 8. These ROC[7] curves show the detection efficiency as a function of decreasing FAR. On the left side of the plot, in the low confidence region both of the pipelines perform the same in that they recover all the injections. Going to the right side of the plot (in the high confidence region), however, the combined pipeline (blue) can recover around 80% to 95% while cWB alone (red) can recover only 0% to 10% of the injected signals. The reason for this lies in the fact that BayesWave gives more significance to the waveform complexity rather than to the signal power. Therefore when introduced to a complex signal, the combined pipeline will claim a higher confidence detection than cWB would do.

2. Sine Gaussians

We studied a total of 1300 injections of sine gaussian injections with different central frequency and quality factors. In Figure 9, we show a scatter plot as in the case of white noise bursts. For sine gaussian injections, we notice that both of the pipelines perform similarly in high confidence regions. Both cWB alone and the combined pipeline recover only the loudest injections. To prove this point further in figure 10 we are showing ROC plots for 5 different sets of Sine Gaussian injections with central frequencies ranging from 70Hz to 361Hz and a quality factor of 9. As before in the lower confidence regions, both the pipelines are able to recover almost 100% of the signals. However, in contrast to the ROC plots of white noise bursts, both the pipelines can recover only 10-20% of the injections in the high confidence regions (the right side on the plot). The reason for this is that sine gaussians are the basis waveforms that reconstruct the signal and glitch models for BayesWave. Therefore when we feed sine gaussian injections to the combined pipeline, BayesWave will consider the waveforms too simple to be proper signals and reject them as glitches in the high confidence regions. Indeed, many of the instrumental artifacts that appear in the LIGO interferometer data are really similar to sine gaussians; thus considering sine gaussians as glitches in the high confidence regions is a fairly safe assumption. However, if there are any astrophysical signals that have sine gaussian waveforms, then the combined pipeline and therefore BayesWave will not be able to detect them.

V. DISCUSSION

Our main purpose in this study was to test the performance of BayesWave in recovering injected signals. To do this, we introduced the combined pipeline which ran cWB as the first stage and BayesWave as a follow-up. We compared the performance of the combined pipeline with that of cWB alone and we understood that the combined pipeline succeeds in recovering complex injections like White Noise Bursts but fails to recover basic waveforms like Sine Gaussians. The reason for this is that BayesWave gives more significance to the waveform complexity rather than to the signal power.

We also studied how well BayesWave could reconstruct the signal by testing whether BayesWave could accu-

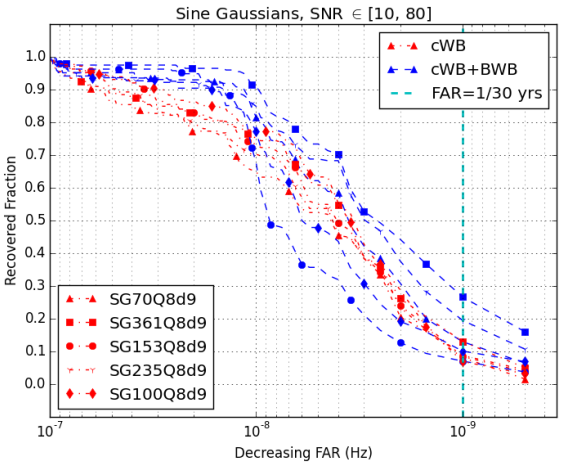

FIG. 10. ROC curves for 5 different sets of White Noise Bursts injections with SNR ranging from 10 to 80. Both of the pipelines perform similarly the high confidence region.

rately recover the injected parameters of the simulated signals. In summary, we understood that BayesWave can succeed in recovering the parameters for Sine Gaussians, but fails to recover the parameters for White Noise Bursts. Our explanation to this phenomenon is the fact that White Noise Bursts are complex, unpolarized signals and as such they tend to be more difficult to model. Sine Gaussians, on the other hand, concur with the types of wavelets that BayesWave uses to fit the data, and as such they are easier to recover. The reason why BayesWave struggles with the parameter recovery of complex injections needs further investigation.

VI. ACKNOWLEDGEMENT

The authors gratefully acknowledge our colleagues at the Albert Einstein Institute in Hanover Germany for creating the dataset and running them through cWB. This project was funded by the National Science Foundation and the LIGO laboratory.

[1] N. J. Cornish and T. B. Littenberg, "Bayeswave: Bayesian inference for gravitational wave bursts and instrument glitches," arXiv preprint arXiv:1410.3835 (2014).

[2] "Wikipedia morlet wavelet," "https://en.wikipedia.org/wiki/Morlet_wavelet", accessed: 2015-07-29.

[3] T. B. Littenberg and N. J. Cornish, "Bayesline: Bayesian inference for spectral estimation of gravitational wave detector noise," arXiv preprint arXiv:1410.3852 (2014).

[4] "Wikipedia reversible-jump markov chain monte carlo," "https://en.wikipedia.org/wiki/Reversible-jump_Markov_chain_Monte_Carlo", accessed: 2015-07-29.

[5] "Coherent WaveBurst background non zero lag - network l1-h1 [64.0-2048.0]," https://atlas3.atlas.aei.uni-hannover.de/~drago/LSC/reports/S6D_BKG_LF_L1H1_2G_rMRA_newreg_gamma0d75/postprod/M1.V_hvetoLH_cat3LH.R_rMRA_hveto_cat3_i0cc70_i0rho0_freq64_2048/, accessed: 2015-07-04.

[6] J. Aasi, J. Abadie, B. Abbott, R. Abbott, T. Abbott, M. Abernathy, T. Accadia, F. Acernese, C. Adams, T. Adams, *et al.*, "Prospects for localization of gravitational wave transients by the advanced ligo and advanced virgo observatories," arXiv preprint arXiv:1304.0670 (2013).

[7] "Wikipedia p-p plot," "https://en.wikipedia.org/wiki/Receiver_operating_characteristic", accessed: 2015-09-01.